Materials Science-Poland, *Vol. 27*, *No. 1*, *2009*

A new composite, Co–Sn metal oxide anode for lithium ion batteries

F. HUANG[1*], X.-Z. LU[1, 2], Y.-F. ZHANG[1], X.-Y. LUO[1], C. YU[1], R. WU[1]

[1]College of Materials Science and Metallurgical Engineering,
Wuhan University of Science and Technology, Wuhan, Hubei, 430081, P.R. China

[2]Wuhan Iron and Steel Mechanic Making Co., Ltd, Wuhan, Hubei, 430083, P.R. China

The structural and morphological evolution of cobalt–tin (Co–Sn) metal composite oxides, synthesized by the decomposition of $CoSn(OH)_6$ precursor at various temperatures, were investigated by X-ray diffraction (XRD) and high-resolution transmission electron microscopy (HRTEM). The precursor was also studied by thermal analysis (TG/DTA). The electrochemical performance of nanosized Co–Sn composite metal oxides was investigated to evaluate their suitability for use as anode materials for Li ion batteries. The results revealed that the samples heat-treated at low temperatures consisted of amorphous $CoSnO_3$, and the samples heat-treated at high temperatures comprised crystalline Co_2SnO_4 and SnO_2. The charge capacity and cyclability were sensitive to the structure and composition of the electrode active materials. The samples heat-treated in the phase transition temperature range exhibited relatively worse electrochemical properties.

Key words: Co–Sn composite oxides; anode materials; lithium ion batteries; liquid precipitating method

1. Introduction

Graphite based anode materials are widely used in commercial lithium ion batteries, owing to their excellent charge and discharge cycling behaviour. However, the theoretical Li storage capacity of graphite is limited to 372 mAh/g [1]. Recently, there has been considerable interest to develop alternative anode materials for lithium ion batteries. Tin oxides have been considered the most promising anode materials for lithium ion batteries, due to their high volumetric and gravimetric capacities [2–4]. According to Courtney and Dahn [5], the reaction of tin oxides with lithium can be described in two steps; for SnO_2, they are:

$$SnO_2 + 4Li^+ + 4e^- \rightarrow 2Li_2O + Sn \quad (1)$$

*Corresponding author, e-mail: hgxlu@163.com

$$Sn + xLi^+ + xe^- \rightarrow Li_xSn \quad (0<x<4.4) \tag{2}$$

Initially, tin oxides are reduced to form small clusters of tin metal, dispersed in a Li_2O framework. Li^+ ions are then reversibly inserted in tin to form Li/Sn alloys. Alloying of Li with tin causes a large volume expansion, leading to cracking of the electrode, and a rapid loss of capacity [5]. The oxides permit the use of Li_2O as a matrix, constraining the volume expansion and contraction [6] during cycling. The cycling performance is enhanced if the active material is finely dispersed in the matrix [7]. Idota et al. [2] suggested a new class of tin-based amorphous composite oxide containing SnO as the active centre for lithium insertion and other glass forming elements such as B, P, Al as an oxide network structure; during charge and discharge, the cyclability of the glass materials had been improved largely.

Recently, Irvine et al. [3, 8, 9] prepared Zn_2SnO_4, Mg_2SnO_4, Co_2SnO_4 and Mn_2SnO_4 spinel metal composite oxides by milling and solid-state reaction at high temperatures. Huang and Yuan [10–13] synthesized a series of amorphous $MgSnO_3$, $CoSnO_3$, $MnSnO_3$ and $ZnSnO_3$ composite metal oxides by the liquid precipitation method and studied their electrochemical properties, in order to try and assess their potential for use as anode materials for lithium ion batteries. In this paper, we report the structural/morphological characteristics and lithium insertion properties of Co–Sn composite metal oxides synthesized from the precursor $CoSn(OH)_6$ by heat-treatment at various temperatures.

2. Experimental

Analytical chemical reagents of Na_2SnO_3 and $CoSO_4$ were used. Solutions of Na_2SnO_3 and $CoSO_4$ in 1:1 molar ratio were mixed under continuous stirring. The pink precipitates were washed with distilled water to remove Na^+ and SO_4^{2-} ions, and then dried in an oven at 120 °C to obtain the pink $CoSn(OH)_6$ precursor. The chemical stoichiometric equation can be expressed as:

$$CoSO_4 + Na_2SnO_3 + 3\ H_2O \rightarrow CoSn(OH)_6 + Na_2SO_4 \tag{3}$$

The precursor powder was heated subsequently at various temperatures for 4 h in air to form Co–Sn metal composite oxide.

Thermogravimetric and differential thermal analyses (TG/DTA) were carried out using a Shimadzu DT-40 thermal analyzer at the heating rate of 10 °C/min in air. XRD was measured on a Shimadzu XRD-6000 diffractometer (Cu-K_α radiation) with the scanning rate of 4°/min, to investigate the phase evolution of $CoSn(OH)_6$ precursor upon heat-treatment at various temperatures. Microstructure (JEM-2100F) of samples was studied by the high-resolution transmission electron microscopy (HRTEM).

The electrochemical cells consisted of a working electrode made of a nanosized Co–Sn metal composite oxides and a counter electrode made of lithium foil. The cells

were assembled in an Ar-filled glove box with both moisture and oxygen concentrations below 5 ppm. The working electrodes were prepared by pressing a film composed of Co–Sn composite metal oxide powders, acetylene black and polytetrafluoroethylene (PTFE) binder (weight ratio of 85:10:5) onto a stainless steel current collector. The electrolyte was 1 M $LiClO_4$ in a mixture of ethylcarbonate (EC) and dimethyl carbonate (DMC) (1:1 in volume ratio), Cellgard 2400 polyethylene was used as the separator. The cells were discharged and charged between 0–2 V versus Li^+/Li at the constant current of 50 mA/g using the Arbin BT 2000 testing system.

3. Results and discussion

3.1. Thermal analysis of the $CoSn(OH)_6$ precursor

The transformation of $CoSn(OH)_6$ precursor during heat-treatment was revealed by DTA and TG data. Figure 1 shows that a sharp endothermic peak occurred on the DTA curve at the temperature of about 300 °C.

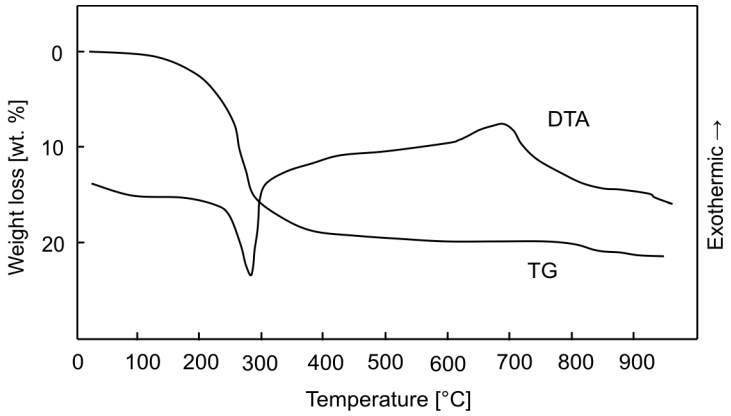

Fig. 1. DTA and TG curves of the $CoSn(OH)_6$ precursor

It also can be seen from the TG curve that the weight loss of the precursor was about 19% in this temperature range, which was due to the reaction:

$$CoSn(OH)_6 \rightarrow CoSnO_3 + 3H_2O \quad (4)$$

The weight loss calculated according to Eq. (4) was 19.3%, which is consistent with the experimental result. A small broad exothermic peak was observed on the DTA curve at the temperature of about 660 °C , but no weight loss was observed from the TG curve at temperatures above 350 °C. This indicates that the phase transition from the amorphous to the crystalline state occurred at this temperature.

3.2. Structural and phase change during heat-treatment

Figure 2 shows the XRD patterns of the $CoSn(OH)_6$ precursor (Fig. 2a) and the final products heat-treated at various temperatures (Fig. 2b). From Figure 2a, it can be seen that there is no evidence of any other phases, as all the diffraction peaks can be indexed for the tetragonal phase $CoSn(OH)_6$ (JCPDS card NO. 20-1455).

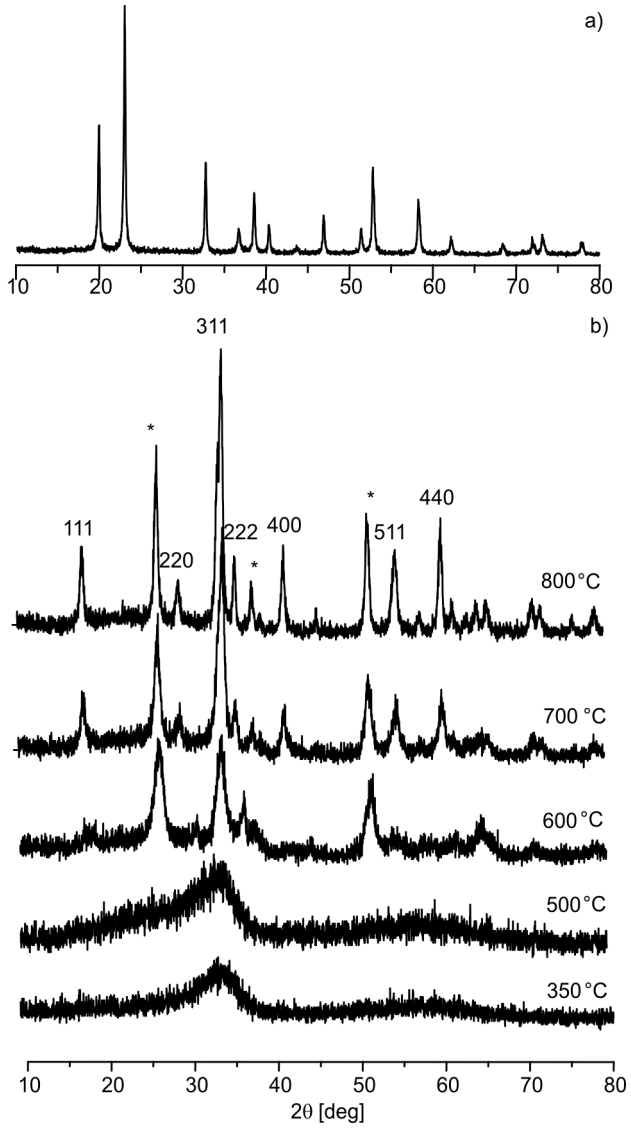

Fig. 2. The XRD patterns of the precursor $CoSn(OH)_6$ (a), and of the final products heat-treated at various temperatures (b). SnO_2 peaks are marked with asterisks

For the samples heat-treated at 350 °C and 500 °C, only one broad peak, related to amorphous $CoSnO_3$, can be observed, and there is no diffraction line assigned to any crystalline phases. This indicates that amorphous or amorphous-like $CoSnO_3$ formed at these temperatures. The XRD patterns shown in Fig. 2b changed sharply after heat-treatment at 600 °C; three diffraction peaks of crystalline SnO_2 were observed, indicating that a phase transition from an amorphous state to a crystalline state occurred during the heat treatment process. However, the XRD peaks of the samples heat-treated at 700 °C were completely different from those of the samples heat-treated at lower temperatures with the appearance of the characteristic peaks of spinel Co_2SnO_4. It suggests that the amorphous $CoSnO_3$ was decomposed spinel Co_2SnO_4 and tetragonal phase SnO_2 when the samples were heated to 700 °C, which is consistent with the results of TG/DTA measurements. In addition, upon further increase in the heat-treatment temperature to 800 °C, the diffraction peaks become stronger and sharper, indicating an increase in the amount of the crystalline phases.

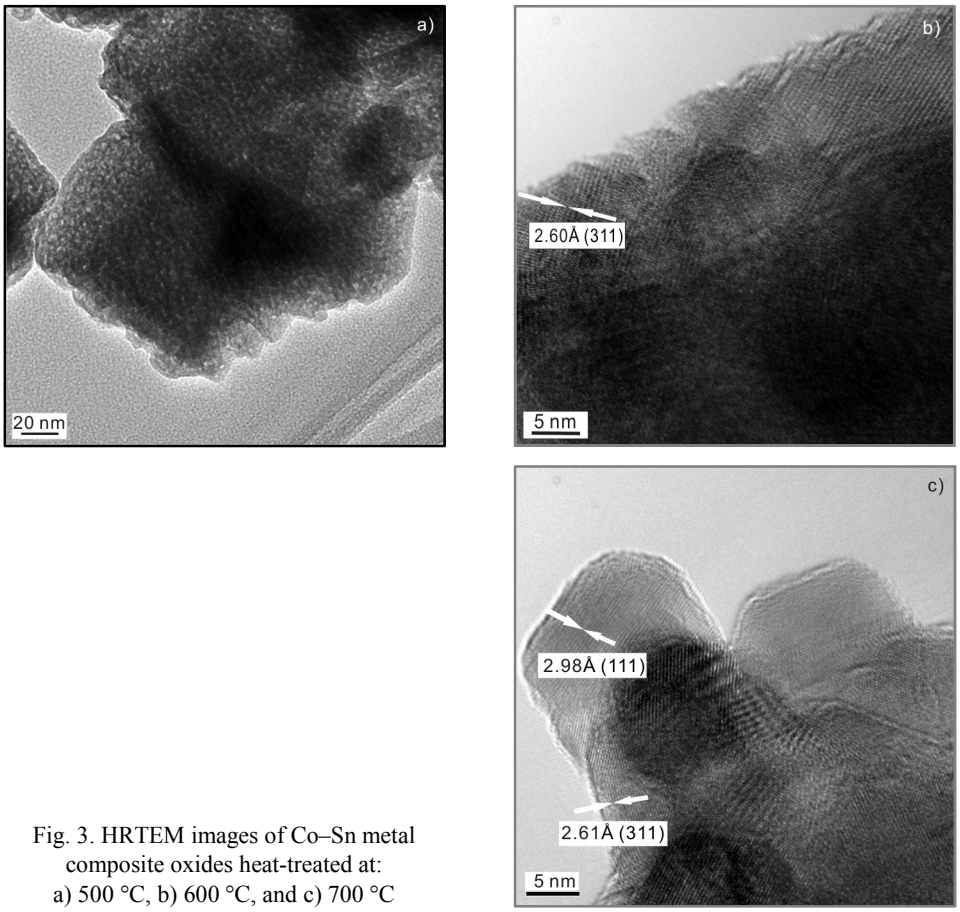

Fig. 3. HRTEM images of Co–Sn metal composite oxides heat-treated at: a) 500 °C, b) 600 °C, and c) 700 °C

Considering all these observations, a three-step process during $CoSn(OH)_6$ heat treatment at various temperatures may be proposed:

$$CoSn(OH)_6 \text{ (crystalline)} \rightarrow CoSnO_3 \text{ (amorphous)} + 3H_2O \quad (5)$$

$$2CoSnO_3 \text{ (amorphous)} \rightarrow Co_2SnO_4 \text{ (amorphous)} + SnO_2 \text{ (crystalline)} \quad (6)$$

$$Co_2SnO_4 \text{ (amorphous)} \rightarrow Co_2SnO_4 \text{ (crystalline)} \quad (7)$$

These results are consistent with the HRTEM images (Fig. 3a–c) showing the structure of nanosized Co–Sn composite oxides samples. The samples after heat-treatment at 500 °C are amorphous $CoSnO_3$, existing as cotton wadding agglomerates. When the heat treatment temperature was increased to 600 °C, the amorphous $CoSnO_3$ was transformed crystalline SnO_2 with the lattice parameter of tin oxide ($d_{hkl}\{311\} = 2.61$ Å) and amorphous Co_2SnO_4 as indicated as some anomalous arranged crystal lattice in the Fig. 3b. 700 °C, more crystalline particles were separated out from the cotton wadding agglomerates with some of the particles showing the lattice parameter of tin oxide ($d_{hkl}\{311\} = 2.61$ Å) and others the lattice parameter of spinel Co_2SnO_4 ($d_{hkl}\{111\} = 2.98$Å). Therefore, the structure and crystal phase of the Co–Sn composite metal oxides are strongly dependent on the heat-treatment temperature of the $CoSn(OH)_6$ precursor.

3.3. Electrochemical performance

First discharge curves of the Li /Co–Sn composite metal oxides cells prepared from the products of $CoSn(OH)_6$ heat-treated at various temperatures are shown in Fig. 4.

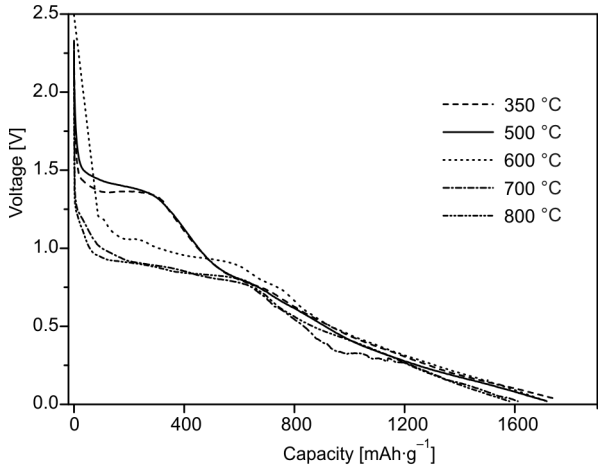

Fig. 4. The first discharge curves of Co–Sn composite oxides heat-treated at various temperatures

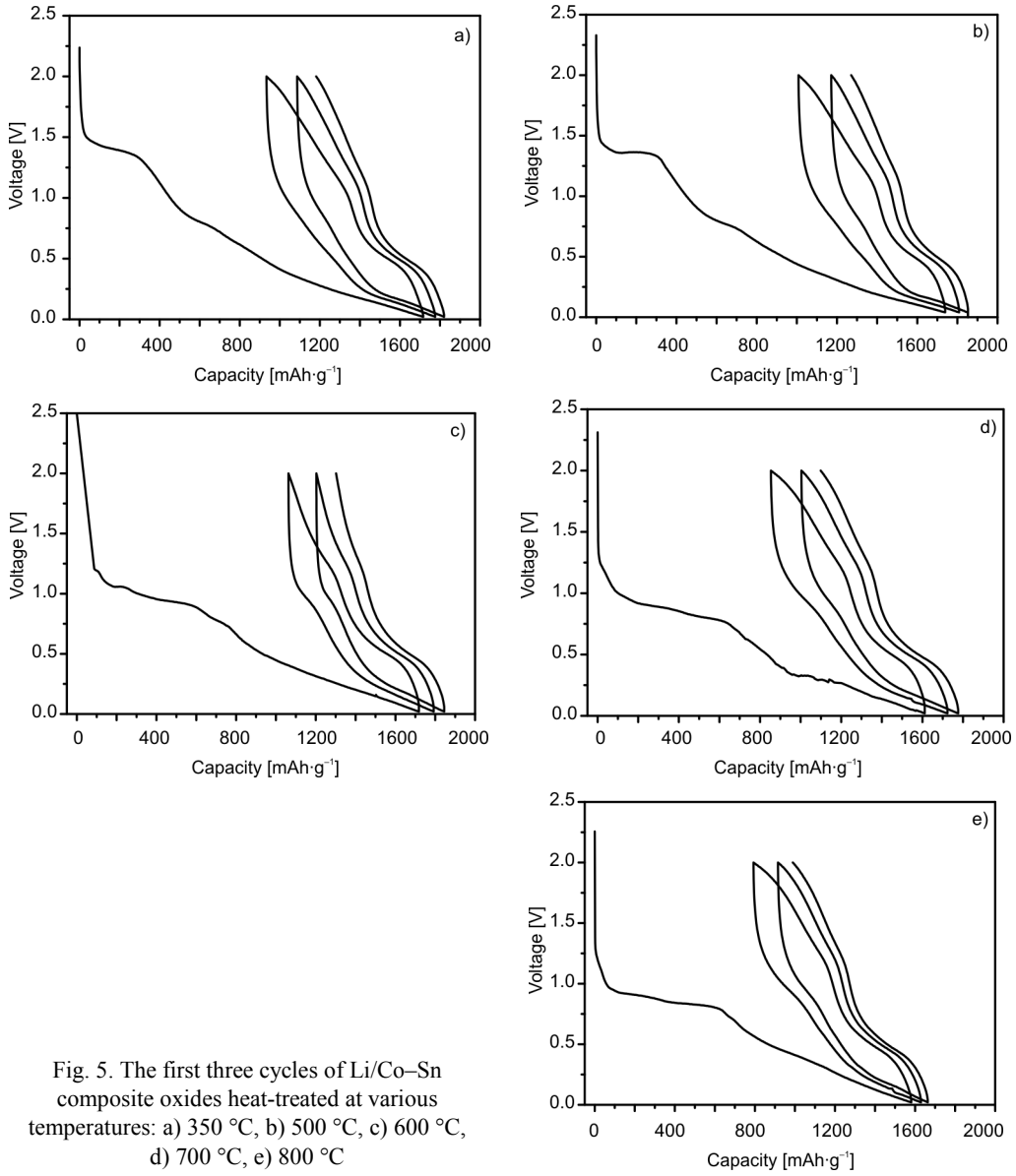

Fig. 5. The first three cycles of Li/Co–Sn composite oxides heat-treated at various temperatures: a) 350 °C, b) 500 °C, c) 600 °C, d) 700 °C, e) 800 °C

Two voltage plateaus at about 1.35 V and 0.8 V, respectively, can be observed in the first discharge curves for the samples heat-treated at 350 °C and 500 °C. With the increase in heat-treatment temperature, only one voltage plateau can be observed, at about 0.95 V, for the samples heat-treated at 600 °C and 700 °C, and two voltage plateaus, at about 0.95 V and 0.4 V, respectively, for the sample heat-treated at 800 °C. Therefore, this suggests that the formation and voltage of the plateau is closely related to the heat-treatment temperature. Figure 5 shows the voltage profiles of the Li/Co–Sn

composite metal oxide cells with $CoSn(OH)_6$ heat-treated at various temperatures for the first three cycles between 0 and 2.0V. For all the samples, the first discharging curves are different from the subsequent discharging curves. After the first cycle, the plateau at about 1.35 V and 0.8 V for the samples heat-treated at 350 °C and 500 °C and the plateau at about 0.9 V for the samples heat-treated at 600 °C, 700 °C and 800 °C all disappeared in the subsequent discharge curves, And the disappearance of the plateau should be responsible for the irreversible capacity [4, 5, 11, 12]. One voltage plateau located at about 0.5 V can be observed clearly in the charging curves for all the samples.

Table 1. Electrochemical properties of the nanosized Co–Sn composite metal oxides formed by heat treatment of $CoSn(OH)_6$ precursor at various temperatures

Property	Heat-treating temperature [°C]				
	350	500	600	700	800
The first discharge capacity [mAh/g]	1739	1716	1718	1612	1581
The first charge capacity [mAh/g]	782	731	655	758	788
Capacity loss in the first cycle [%]	55.0	57.4	61.9	53.0	50.1
$R_{20/1}$ [%]	45.4	39.4	32.7	48.3	50.5

Table 1 shows the relationship between the electrochemical properties of all Co–Sn composite metal oxides and the heat treatment temperature of $CoSn(OH)_6$. It can be seen that as the heat treatment temperature increases, the first discharge specific capacity of Co–Sn composite oxides anodes decreases. However, the lowest initial charge specific capacity obtained was as high as 655 mAh/g for the sample heat-treated at 600 °C. This is much higher than the theoretical capacity of graphite (372 mAh/g). However, for the Co–Sn composite metal oxide anodes, the problem associated with other tin oxide based systems exists, i.e. about half of the initial lithium capacity is lost due to irreversible changes in the oxide matrix. To help quantify the cycling stability of various samples, a parameter called the capacity retention index $R_{20/1}$is defined. This parameter is the capacity in the 20th charge cycle divided by the capacity in the first charge cycle. Cells that cycle without capacity loss, therefore, will have $R_{20/1}$ equal to unity [14]. As can be seen in Table 1, the samples heat-treated at the phase transition temperature (600 °C) exhibited poorer cycling performance. Taking into account all the above results, it is certain that the samples heat-treated at phase transition temperature range exhibit relatively worse electrochemical properties.

The differential capacity plots obtained at the first cycle for all Co–Sn composite metal oxide samples heat-treated at various temperatures are shown in Fig. 6. Two cathodic peaks at about 1.35 V and 0.8 V, respectively, can be observed for the samples heat-treated at 350 °C and 500 °C. Only one cathodic peak occurring at about 0.95 V can be observed for the samples heat-treated at higher temperatures (600 °C, 700 °C and 800 °C). Compared with the results published in Refs [3, 14], it

can be concluded that the change in cathodic peaks positions is due to the formation of the spinel Co_2SnO_4 phase seen from XRD patterns.

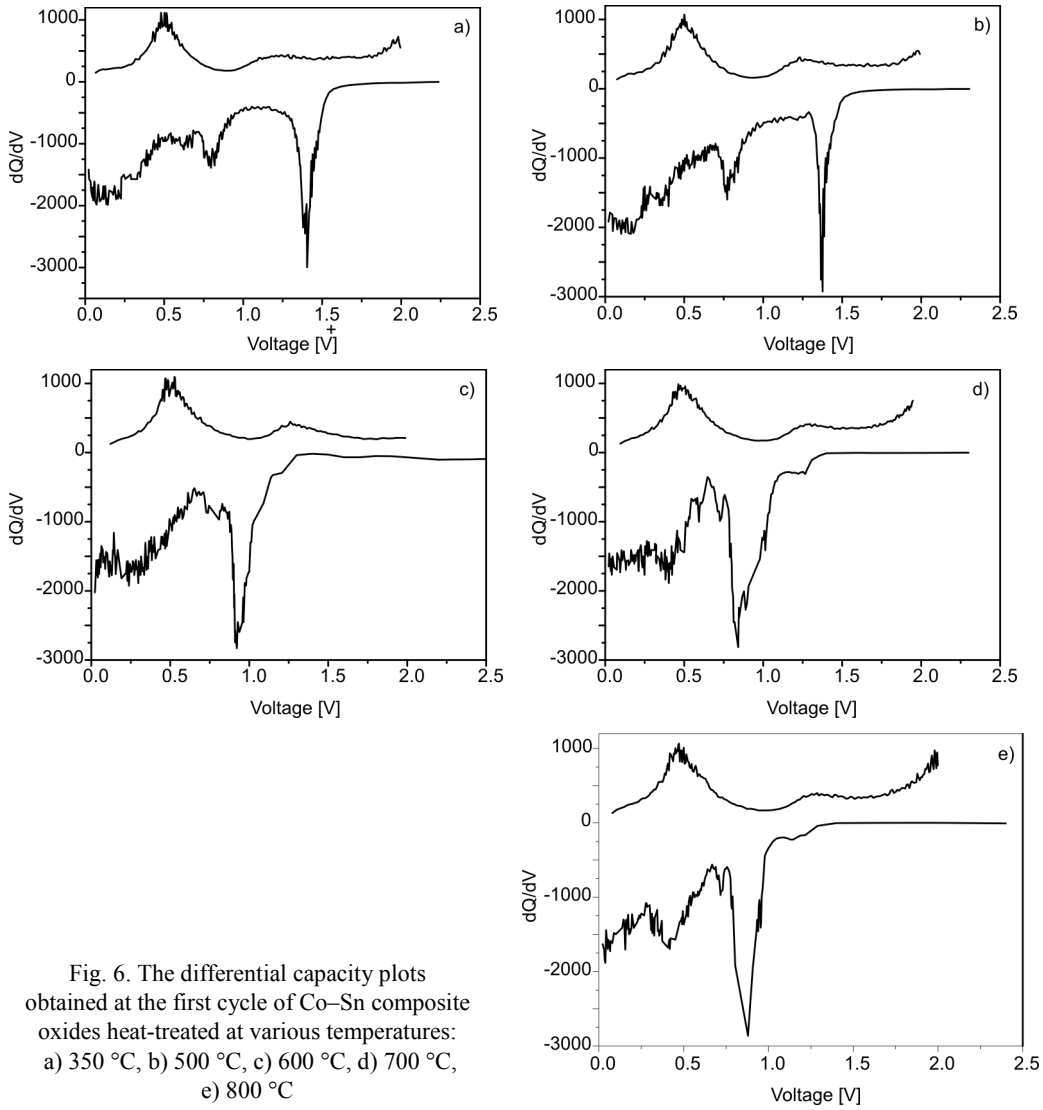

Fig. 6. The differential capacity plots obtained at the first cycle of Co–Sn composite oxides heat-treated at various temperatures: a) 350 °C, b) 500 °C, c) 600 °C, d) 700 °C, e) 800 °C

For all the samples, there are two anodic peaks located at about 0.5 V and 1.25 V, respectively, suggesting that, besides the alloying reaction involving Sn and Li, Co also participated in the electrode reaction [15]. All the anodic and cathodic peaks in differential capacity plots are consistent with the voltage plateaus in the charge and discharge curves. In addition, the shape of cathodic peaks for the 350 °C and 500 °C heat-treated samples is different from the shape of cathodic peaks for the samples heat-treated at higher temperatures. At the stage of phase transition from amorphous to

crystalline state or at the formation stage of the new phase, non uniform particle distribution results in worse electrochemical characteristics. Therefore it is believed that the phase transition is responsible for the worse electrochemical performance of the cells.

4. Conclusions

A series of nano-sized Co–Sn composite metal oxides have been prepared by heat treatment of $CoSn(OH)_6$ precursor at various temperatures. With the increase in temperature, $CoSn(OH)_6$ decomposes to form amorphous $CoSnO_3$ firstly, which is progressively converted to crystalline Co_2SnO_4 and SnO_2. The electrochemical characteristics of these composite oxides as anode materials for lithium ion batteries are closely related to their structure and composition. In the phase transition process, slight changes in temperature can greatly alter the electrochemical performance. The Co–Sn composite oxides show good possibilities as anode materials for lithium ion batteries. Future work should focus on the reaction processes involving lithium and anode materials, and on reducing the problem of irreversible changes.

Acknowledgement

This work was supported by the Natural Science Foundation of Hubei Province (No. 2007ABA320) and National 973 key research program.

References

[1] YING Z., JUN Y., WANG J.L, . Electrochim. Acta, 52 (2007), 5863.
[2] IDOTA Y., KUBOTA T., MATSUFUJI A., MACKAWA Y., Science, 276 (1997), 1395.
[3] BELLIARD F., CONNOR P.A., IRVINE J.T.S., Solid State Ionics, 135 (2000), 163.
[4] YUAN Z.Y., HUANG F., SUN J.X., ZHOU Y.H., Chem. Lett., 3 (2002), 408.
[5] COURTNEY L.A., DAHN J.R., J. Electrochem. Soc., 144 (1997), 2943.
[6] WINTER M., BESENHARD J.O., Electrochim. Acta, 45 (1999), 31.
[7] LI H., HUANG X.J., CHEN L.Q., Electrochem. Solid-State Lett., 1 (1998), 241
[8] BELLIARD F., IRVINE J.S., J. Power Sources, 97–98 (2001), 219.
[9] CONNOR P.A., BELLIARD F., IRVINE J.S., J. Power Sources, 97–98 (2001), 223.
[10] YUAN Z.Y., HUANG F., SUN J.X., ZHOU Y.H., Chem. Lett., 3 (2002), 408.
[11] HUANG F., YUN Z.Y., ZHAN H., YUAN Z.Y., SUN J.T., Mater. Lett., 57 (2003), 3341.
[12] HUANG F., YUAN Z.Y., ZHAN H., YUAN Z.Y., Mater. Chem. Phys., 83 (2004), 16.
[13] YUAN Z.Y., HUANG F., FENG C.Q., J. Mater. Sci. Lett., 22 (2003), 143.
[14] MAO O., TURNER, R.L., COURTNEY L.A., FREDERICKSEN B.D., DAHN J.R., Electrochem. Solid-State Lett., 2 (1999), 3.
[15] HUANG F., ZHAN H., YUAN Z.Y., Chinese J. Chem., 21 (2003), 1275.

Received 17 March 2008
Revised 7 August 2008